Near-Real-Time NOAA/NSIDC Climate Data Record of Passive Microwave Sea Ice Concentration, Version 1

USER GUIDE

How to Cite These Data

As a condition of using these data, you must include a citation:

Meier, W. N., F. Fetterer, and A. K. Windnagel. 2017. *Near-Real-Time NOAA/NSIDC Climate Data Record of Passive Microwave Sea Ice Concentration, Version 1*. [Indicate subset used]. https://doi.org/10.7265/N5FF3QJ6. [Date Accessed].

FOR QUESTIONS ABOUT THESE DATA, CONTACT NSIDC@NSIDC.ORG

FOR CURRENT INFORMATION, VISIT https://nsidc.org/data/G10016

National Snow and Ice Data Center

TABLE OF CONTENTS

1 DATA DESCRIPTION

1.1 Summary

The Near-Real-Time NOAA/NSIDC Climate Data Record of Passive Microwave Sea Ice Concentration (NRT CDR) data set is the daily-update version of the *NOAA/NSIDC Climate Data Record of Passive Microwave Sea Ice Concentration* (final CDR). The NRT CDR fills the temporal gap between updates of the final CDR, occurring roughly annually, and provides the most recent data. The NRT CDR is preliminary and uses input data that do not go through the same quality control measures as for the final CDR. When the final CDR receives an update, users should download the latest update to replace any NRT data they may be using. To be notified of final CDR updates, please register for the data set mailing list on the final CDR Registration page.

The major differences between the final CDR and this NRT CDR are the following:

- The NRT CDR uses brightness temperature data from a different source than the final CDR. The NRT CDR uses the *Near-Real-Time DMSP SSM/I-SSMIS Daily Polar Gridded Brightness Temperatures* (NSIDC-0080) data set whereas the final CDR uses the *DMSP SSM/I-SSMIS Daily Polar Gridded Brightness Temperatures* (NSIDC-0001) data set. NSIDC-0001 brightness temperatures are supplied to NSIDC by Remote Sensing Systems (RSS), and undergo stringent quality control. NSIDC-0080 relies on brightness-temperature swath data from NOAA Comprehensive Large Array-Data Stewardship System (CLASS) that are available in near-real time. For complete details on the differences in these two input data sets, please view their respective data set user guides.
- The NRT CDR does not contain the three ancillary Goddard Space Flight Center (GSFC) concentration variables. For the daily resolution data, the variables omitted are `goddard_merged_seaice_conc`, `goddard_nt_seaice_conc`, and `goddard_bt_seaice_conc`. For the monthly resolution data, the variables omitted are `goddard_merged_seaice_conc_monthly`, `goddard_nt_seaice_conc_monthly`, and `goddard_bt_seaice_conc_monthly`.

The Near-real-time NOAA/NSIDC sea ice concentration Climate Data Record (CDR) is produced using an algorithm that joins ice concentrations from two well established algorithms developed at the NASA Goddard Space Flight Center (GSFC): the NASA Team (NT) algorithm (Cavalieri et al. 1984) and the Bootstrap (BT) algorithm (Comiso 1986). The CDR algorithm then blends the NT and BT output concentrations by selecting, for each grid cell, the higher concentration value. The NT and BT algorithms are run at NSIDC as part of CDR processing; these output concentrations are intermediate products that are not saved. For a high-level overview of the CDR algorithm, see the Summary of the *NOAA/NSIDC Climate Data Record of Passive Microwave Sea Ice Concentration* User Guide.

The data are on the NSIDC polar stereographic grid with nominal 25 x 25 km grid cells and are available in NetCDF4 CF-1.6 file format. Both monthly and daily resolution files include four different sea ice concentration variables. One variable is the primary NRT NOAA/NSIDC CDR sea ice concentrations: `seaice_conc_cdr` for daily and `seaice_conc_monthly_cdr` for monthly. Variables containing standard deviation, quality flags, and projection information are also included in the NetCDF4 files.

1.2 Parameters

The parameter of this data set is sea ice concentration which is the fraction of ocean area covered by sea ice. Sea ice concentration represents an areal coverage of sea ice. For a given grid cell, the parameter provides an estimate of the fractional amount of sea ice covering that cell, with the remainder of the area consisting of open ocean. Land areas are coded with a land mask value.

1.3 File Information

1.3.1 Format

These data are provided in NetCDF4 file format and are compliant with the Climate and Forecast (CF) Metadata Convention CF-1.6 (Eaton et al. 2010).

Both the daily and monthly files contain 13 variables that are described in the sections 1.3.2.1 Daily File Variable Description and 1.3.2.2 Monthly File Variable Description.

1.3.2 File Contents

1.3.2.1 Daily File Variable Description

The daily NetCDF4 files contain 13 variables. Table 1 provides a quick look at these variables with links to more detailed information.

Table 1. Daily Variables at a Glance. Click Variable Name for More Information.

Variable Name	Brief Description	Variable Name	Brief Description
seaice_conc_cdr	NRT NOAA/NSIDC daily sea Ice CDR.	time	Time in days since 1601-01-01 00:00:00.
stdev_of_seaice_conc_cdr	Standard deviation for the daily NRT NOAA/NSIDC CDR sea ice concentration.	xgrid	X-offset in meters of the projection grid centers.

Variable Name	Brief Description	Variable Name	Brief Description
melt_onset_day_seaice_conc_cdr	The day of year on which melting sea ice was first detected in each grid cell for the daily NRT NOAA/NSIDC CDR.	ygrid	Y-offset in meters of the projection grid centers.
qa_of_seaice_conc_cdr	A number of different quality flags related to the daily NRT NOAA/NSDIC CDR.	latitude	Latitude in degrees north of the projection grid centers.
projection	Projection information for the data.	longitude	Latitude in degrees north of the projection grid centers.

seaice_conc_cdr

Description NOAA/NSIDC CDR sea ice concentrations which is the fraction of ocean area covered by sea ice that span 1987 through most recent processing. This variable is merged from the NASA Team processed sea ice concentrations and Bootstrap processed sea ice concentrations using the CDR Algorithm. For a description of the algorithm used to merge these, see section 2.2.2 CDR Algorithm. Note that the 1978 to 1987 data files contain this variable, but they are populated with a fill value of 255. See Table 2 for a list of all flag values.

Data Type Byte array with dimensions [304, 448, 1] (North) and [316, 332, 1] (South), which are the xgrid, ygrid, and time, respectively.

Valid Range 0 to 1. Note: Byte values are actually stored in the files from 0 to 100 but are presented by most, but not all, NetCDF readers as values ranging from 0 to 1 because of a scaling factor attribute (`scale_factor`) for this variable of .01 that is applied by most NetCDF readers.

Attributes `_FillValue, valid_range, _Unsigned, long_name, standard_name, units, scale_factor, coordinates, flag_values, flag_meanings, datum, grid_mapping, reference, ancillary_variables`

Fill Value 255

Units Unitless

Table 2. Flag Values for Sea Ice Concentration Variables

Flag Name	Value
Northern Hemisphere pole hole (the region around the pole not imaged by the sensor)	251
Lakes	252
Coast/Land adjacent to ocean	253
Land	254
Missing/Fill	255

stdev_of_seaice_conc_cdr

Description Standard deviation for the daily NRT NOAA/NSIDC CDR sea ice concentration. This value is the standard deviation of a given grid cell along with its eight surrounding grid cells (for nine values total) from both the NASA Team and Bootstrap data. This means that the standard deviation is computed using a total of 18 values: nine from the intermediate NISDC NASA Team data and nine from the intermediate NSIDC Bootstrap data. Grid cells with high standard deviations indicate values with lower confidence levels.

Data Type Float array with dimensions [304, 448, 1] (North) and [316, 332, 1] (South), which are the xgrid, ygrid, and time, respectively.

Valid Range 0.0 to 1.0

Attributes `_FillValue, valid_range, long_name, units, coordinates, missing_value, datum, grid_mapping`

Fill Value -1.0

Units 1

melt_onset_day_seaice_conc_cdr

Description Contains the day of year on which melting sea ice was first detected in each grid cell. Once detected, the value is retained for the rest of the year. For example, if a grid cell started melting on day 73, the variable for the grid cell on that day will be 73, as will all subsequent days until the end of the year. The melt onset day is only calculated for the melt season: days 60 through 244, inclusive. Before melting is detected or if melt is never detected for that grid cell, the value will be -1 (missing / fill value).

Data Type Integer array with dimensions [304, 448, 1] (North) and [316, 332, 1] (South), which are the xgrid, ygrid, and time, respectively.

Valid Range 60 to 244

Attributes	`_FillValue, valid_range, _Unsigned, long_name, standard_name, units, coordinates, missing_value, datum, grid_mapping`
Fill Value	-1
Units	Unitless

qa_of_seaice_conc_cdr

Description	A number of different quality flags related to the daily NRT NOAA/NSDIC CDR sea ice concentration. See Table 3 for a list of the flags. **Note**: Grid cells that meet multiple conditions will have a value that is the sum of the values of each individual condition. For example, if the byte value for a cell is 129, both the `melt_start_detected` flag and `BT_source_for_CDR` flag have been set.
Data Type	Byte array with dimensions [304, 448, 1] (North) and [316, 332, 1] (South), which are the xgrid, ygrid, and time, respectively.
Valid Range	1 to 255
Attributes	`_FillValue, valid_range, _Unsigned, long_name, standard_name, units, coordinates, flag_masks, flag_meanings, missing_value, datum, grid_mapping`
Fill Value	0
Units	Unitless

Table 3. Daily QA Flag Values

Condition	Flag Value	NetCDF Variable Name	Description
BT source for CDR (BT > NT)	1	BT_source_for_CDR	Indicates that the value from the Bootstrap algorithm was greater than the NASA Team algorithm, thus the Bootstrap value was used for this grid cell.
NT source for CDR (NT > BT)	2	NT_source_for_CDR	Indicates that the value from the NASA Team algorithm was greater than the Bootstrap algorithm, thus the NASA Team value was used for this grid cell.
Region masked by ocean climatology	4	no_ice_allowed_per_climatology	Indicates that this grid cell has been designated as ocean via an ocean mask or valid ice mask.

Condition	Flag Value	NetCDF Variable Name	Description
Grid cell near the coast	8	grid_cell_near_to_coast	Indicates that this grid cell is located near the coastline, so it may be less reliable and of lower quality than cells further from the coast.
Concentration < 50%	32	concentration_below_fifty_percent	Indicates that the concentration value for this grid cell is under 50%. This is important because the NASA Team and Bootstrap algorithms do not pick up low concentration ice very well and also confuse low concentration with thin ice. Therefore, these grid cells have a lower confidence level.
Start of Melt Detected (Arctic only)	128	melt_start_detected	Indicates that the ice in this grid cell has shown evidence of starting to melt, so values may be less reliable. The melt onset test is used starting on March 1 (DOY=60), around the time when the maximum sea ice extent is reached each year. Once a grid cell is flagged as melting, it remains so through the rest of the summer until September 1 (DOY=244), roughly the time when extent reaches its minimum value. When the sea ice concentration is zero, the flag will be turned off.

projection

Description Provides details about the polar stereo projection information for the data.

Data Type Char array with dimension [304] (North) and [316] (South)

Valid Range N/A

Attributes `grid_boundary_top_projected_y`, `grid_boundary_bottom_projected_y`, `grid_boundary_right_projected_x`, `grid_boundary_left_projected_x`, `parent_grid_cell_row_subset_start`, `parent_grid_cell_row_subset_end`,

	`parent_grid_cell_column_subset_start, parent_grid_cell_column_subset_end, spatial_ref, proj4text, srid, GeoTransform, grid_mapping_name, latitude_of_projection_origin, standard_parallel, straight_vertical_longitude_from_pole, longitude_of_projection_origin, scaling_factor, false_easting, false_northing , semimajor_radius, semiminor_radius, units`
Fill Value	N/A
Units	Meters

time

Description	Time in days since 1601-01-01 00:00:00.
Data Type	Double
Valid Range	N/A
Attributes	`standard_name, units, long_name, calendar, axis`
Fill Value	N/A
Units	Days since 1601-01-01 00:00:00

xgrid

Description	X-offset in meters of the projection grid centers.
Data Type	Float array with dimension [304] (North) and [316] (South)
Valid Range	-3.85000e+006 to 3.75000e+006
Attributes	`valid_range, units, long_name, standard_name, axis`
Fill Value	N/A
Units	Meters

ygrid

Description	Y-offset in meters of the projection grid centers.
Data Type	Float array with dimension [448] (North) and [332] (South)
Valid Range	-5.35000e+006 to 5.85000e+006
Attributes	`valid_range, units, long_name, standard_name, axis`
Fill Value	N/A
Units	Meters

latitude

Description	Latitude in degrees north of the projection grid centers.
Data Type	Double array with dimensions [304, 448] (North) and [316, 332] (South)
Valid Range	0.0 to 90.0 for northern hemisphere files, and -90.0 to 0.0 for southern hemisphere files.
Attributes	`standard_name, long_name, units, valid_range, _FillValue`
Fill Value	-999
Units	Degrees north

longitude

Description	Longitude in degrees east of the projection grid centers.
Data Type	Double array with dimensions [304, 448] (North) and [316, 332] (South)
Valid Range	-180.0 to 180.0
Attributes	`standard_name, long_name, units, valid_range, _FillValue`
Fill Value	-999
Units	Degrees east

1.3.2.2 Monthly File Variable Description

The monthly NetCDF4 files contain 13 variables. Table 4 provides a quick look at these variables with links to more detailed information.

Note: The global attributes for the monthly data files erroneously say that the sensor platform is DMSP F17. However, this can be ignored; files downloaded from this data set use the DMSP F18 platform. The global attributes will be updated in a future release.

Table 4. Monthly Variables at a Glance. Click Variable Name for More Information.

Variable Name	Brief Description	Variable Name	Brief Description
seaice_conc_monthly_cdr	NRT NOAA/NSIDC monthly sea Ice CDR.	time	Time in days since 1601-01-01 00:00:00.
stdev_of_seaice_conc_monthly_cdr	Standard deviation for the monthly NRT NOAA/NSIDC CDR sea ice concentration.	xgrid	X-offset in meters of the projection grid centers.
melt_onset_day_seaice_conc_monthly_cdr	The day of year on which melting sea ice was first detected in each grid cell for the monthly NRT NOAA/NSIDC CDR.	ygrid	Y-offset in meters of the projection grid centers.
qa_of_seaice_conc_monthly_cdr	A number of different quality flags related to the monthly NRT NOAA/NSDIC CDR.	latitude	Latitude in degrees north of the projection grid centers.
projection	Projection information for the data.	longitude	Latitude in degrees north of the projection grid centers.

seaice_conc_monthly_cdr

Description	The monthly average of the NRT CDR sea ice concentrations (`seaice_conc_cdr`). See Table 2 for a list of flag values used in this variable.
Data Type	Byte array with dimensions [304, 448, 1] (North) and [316, 332, 1] (South), which are the xgrid, ygrid, and time, respectively.
Valid Range	0 to 1. Note: Byte values are actually stored in the files from 0 to 100 but are presented by most, but not all, NetCDF readers as values ranging from 0 to 1 because of a scaling factor attribute (`scale_factor`) for this variable of .01 that is applied by most NetCDF readers.
Attributes	`_FillValue, valid_range, _Unsigned, long_name, standard_name, units, scale_factor, coordinates, flag_values, flag_meanings, datum, grid_mapping, reference, ancillary_variables`
Fill Value	255
Units	Unitless

stdev_of_seaice_conc_monthly_cdr

Description	Standard deviation for the monthly NRT NOAA/NSIDC CDR sea ice concentration variable (`seaice_conc_monthly_cdr`). This value is the standard deviation of the concentration of all daily values for the month at that grid cell.
Data Type	Float array with dimensions [304, 448, 1] (North) and [316, 332, 1] (South), which are the xgrid, ygrid, and time, respectively.
Valid Range	0.0 to 1.0
Attributes	`_FillValue, valid_range, long_name, units, coordinates, missing_value, datum, grid_mapping`
Fill Value	-1.0
Units	Unitless

melt_onset_day_seaice_conc_monthly_cdr

Description	Contains the day of year on which melting sea ice was first detected in each grid cell. Once detected, the value is retained for the rest of the year. For example, if a grid cell started melting on day 73, the variable for the grid cell on that day will be 73, as will all subsequent days until the end of the year. The melt onset day is only calculated for the melt season: days 60 through 244, inclusive. Before melting is detected or if melt is never detected for that grid cell, the value will be -1 (missing / fill value).
Data Type	Integer array with dimensions [304, 448, 1] (North) and [316, 332, 1] (South), which are the xgrid, ygrid, and time, respectively.
Valid Range	60 to 244
Attributes	`_FillValue, valid_range, _Unsigned, long_name, standard_name, units, coordinates, missing_value, datum, grid_mapping`
Fill Value	-1
Units	Unitless

qa_of_seaice_conc_monthly_cdr

Description	A number of different quality flags related to the monthly NRT NOAA/NSDIC CDR sea ice concentration variable (`seaice_conc_monthly_cdr`). See Table 5 for a list of the monthly flags. **Note**: Grid cells that meet multiple conditions will have a value that is the sum of the values of each individual condition. For example, if the byte value for a cell is 129, both the `melt_detected_greater_than_half_month` flag and `BT_majority_algorithm_for_monthly_CDR` flag have been set.

Data Type	Byte array with dimensions [304, 448, 1] (North) and [316, 332, 1] (South), which are the xgrid, ygrid, and time, respectively.
Valid Range	1 to 255
Attributes	`_FillValue, valid_range, _Unsigned, long_name, standard_name, units, coordinates, flag_masks, flag_meanings, missing_value, datum, grid_mapping`
Fill Value	0
Units	Unitless

Table 5. Monthly QA Flag Values

Condition	Flag Value	NetCDF Variable Name	Description
Number of BT > Number of NT	1	BT_majority_algorithm_for_monthly_CDR	Indicates that the majority of the values used for the monthly average, at this grid cell, are from the Bootstrap algorithm.
Number of NT > Number of BT	2	NT_majority_algorithm_for_monthly_CDR	Indicates that the majority of the values used for the monthly average, at this grid cell, are from the NASA Team algorithm.
Region masked by ocean climatology	4	no_ice_allowed_per_climatology	Indicates that this grid cell has been designated as ocean via an ocean mask or valid ice mask.
Grid cell near the coast	8	grid_cell_near_to_coast	Indicates that this grid cell is located near the coastline, so it may be less reliable and of lower quality.
Ice present < 50%	32	ice_present_less_half_of_month	Indicates that for this grid cell ice was present less than half of the month, so the value is more likely due to a temporal difference of the concentration than a spatial one.

Condition	Flag Value	NetCDF Variable Name	Description
melt detected >= 1	64	melt_detected_at_least_one_day	Indicates that for this grid cell melt was detected at least one day during the month, so it may be less reliable and of lower quality.
Melt detected > 50%	128	melt_detected_greater_than_half_month	Indicates that for this grid cell melt was detected at least half of the days during the month, so it may be even less reliable and of lower quality than for those with melt detected less than half the month or not at all.

projection

Description	Provides details about the polar stereo projection information for the data.
Data Type	Char array with dimension [304] (North) and [316] (South)
Valid Range	N/A
Attributes	`grid_boundary_top_projected_y, grid_boundary_bottom_projected_y, grid_boundary_right_projected_x, grid_boundary_left_projected_x, parent_grid_cell_row_subset_start, parent_grid_cell_row_subset_end, parent_grid_cell_column_subset_start, parent_grid_cell_column_subset_end, spatial_ref, proj4text, srid, GeoTransform, grid_mapping_name, latitude_of_projection_origin, standard_parallel, straight_vertical_longitude_from_pole, longitude_of_projection_origin, scaling_factor, false_easting, false_northing , semimajor_radius, semiminor_radius, units`
Fill Value	N/A
Units	Meters

time

Description	Time in days since 1601-01-01 00:00:00.
Data Type	Double
Valid Range	N/A
Attributes	`standard_name, units, long_name, calendar, axis`
Fill Value	N/A
Units	Days since 1601-01-01 00:00:00

xgrid

Description	X-offset in meters of the projection grid centers.
Data Type	Float array with dimension [304] (North) and [316] (South)
Valid Range	-3.85000e+006 to 3.75000e+006
Attributes	`valid_range, units, long_name, standard_name, axis`
Fill Value	N/A
Units	Meters

ygrid

Description	Y-offset in meters of the projection grid centers.
Data Type	Float array with dimension [448] (North) and [332] (South)
Valid Range	-5.35000e+006 to 5.85000e+006
Attributes	`valid_range, units, long_name, standard_name, axis`
Fill Value	N/A
Units	Meters

latitude

Description	Latitude in degrees north of the projection grid centers.
Data Type	Double array with dimensions [304, 448] (North) and [316, 332] (South)
Valid Range	0.0 to 90.0 for northern hemisphere, and -90.0 to 0.0 for southern hemisphere.
Attributes	`standard_name, long_name, units, valid_range, _FillValue`
Fill Value	-999.0
Units	Degrees north

longitude

Description	Longitude in degrees east of the projection grid centers.
Data Type	Double array with dimensions [304, 448] (North) and [316, 332] (South)
Valid Range	-180.0 to 180.0
Attributes	`standard_name, long_name, units, valid_range, _FillValue`
Fill Value	-999.0
Units	Degrees east

1.3.3 Directory Structure

The data files are organized on the FTP site into two main directories by hemisphere: `north` and `south`. Within each of these, there are three sub-directories: `checksums`, `daily`, and `monthly`. The checksums directory contains md5 checksums of the daily and monthly data files to ensure accuracy in data transfer. The daily directory is further sub-divided into directories labeled by the 4-digit year (YYYY) beginning with 1978; the daily files reside within their respective year directory. All of the monthly files reside directly in the monthly directory.

1.3.4 Naming Convention

The file naming convention for the daily and monthly files is listed below and described in Table 6:

Daily: `seaice_conc_daily_icdr_hh_sat_yyyymmdd_vXXrXX.nc`

Monthly: `seaice_conc_monthly_icdr_hh_sat_yyyymm_vXXrXX.nc`

Where:

Table 6. File Naming Convention

Variable	Description
seaice_conc	Identifies files containing sea ice concentration data
daily	Identifies files containing daily sea ice concentration
monthly	Identifies files containing monthly sea ice concentration
hh	Hemisphere (nh: North, sh: South)
sat	Satellite the data came from (f18: DMSP F18)
yyyy	4-digit year
mm	2-digit month
dd	2-digit day of month
vXXrXX	Version and release number of the data file (v01r00: Version 1, Release 0)
.nc	Identifies a NetCDF file
.nc.mnf	Identifies this as an md5 checksum file

1.4 Spatial Information

1.4.1 Coverage and Resolution

These data cover both the Northern and Southern polar regions at a 25 x 25 km grid cell size. Note: While resolution and grid cell size are often used interchangeably with regards to satellite data, there is an important difference. Resolution refers more properly to the instantaneous field of view (IFOV) of a particular sensor frequency. That is, resolution is the spot size on the ground that the sensor channel can resolve. The SSMIS channels used are the 19 GHz vertical, the 19 GHz horizontal, and the 37 GHz vertical. The IFOV of the 19 GHz SSMIS passive microwave channel is approximately 70 km x 45 km. See Table 12 for a complete list of IFOVs by channel.

Since these data are gridded onto a 25 x 25 km grid and the IFOV of the sensor is coarser than this, the sensor is obtaining information from up to a 3 x 2 grid cell (~75 km x 45 km) region, but because a simple drop-in-the-bucket gridding method is used, that signature is placed in a single grid cell. This results in a spatial "smearing" across several grid cells. Also, some grid cells do not coincide with the center of the sensor footprint and are thus left as missing even though there is brightness temperature information available at that region. Higher frequency channels have finer resolution, but because the sea ice concentration algorithms use data from the 19 GHz channel, the sea ice concentration estimate is affected by the makeup of the surface over an area considerably larger than the nominal 25 km resolution.

The spatial coordinates for the Northern polar region are the following:

Southernmost Latitude: 31.10° N
Northernmost Latitude: 89.84° N
Westernmost Longitude: 180° W
Easternmost Longitude: 180° E

The spatial coordinates for the Southern polar region are the following:

Southernmost Latitude: 89.84° S
Northernmost Latitude: 39.36° S
Westernmost Longitude: 180° W
Easternmost Longitude: 180° E

1.4.2 Projection and Grid Description

The sea ice concentration data are displayed in a polar stereographic projection. For more information on this projection, see the NSIDC Polar Stereographic Projections and Grids Web page. Note that the polar stereographic grid is not equal area; the latitude of true scale (tangent of the planar grid) is 70 degrees. The grid size varies depending on the region, as shown in Table 7.

Table 7. Polar Stereo Grid Size

Region	Columns	Rows
North	304	448
South	316	332

1.5 Temporal Coverage and Resolution

The NRT CDR sea ice concentrations span the end of the temporal coverage of the final CDR (G02202) to the present; provided at both a daily resolution and a monthly averaged resolution.

2 DATA ACQUISITION AND PROCESSING

2.1 Acquisition

The input gridded brightness temperatures used for creating the NRT CDR sea ice concentrations come from NSIDC in the *Near-Real-Time DMSP SSM/I-SSMIS Daily Polar Gridded Brightness Temperatures* data set. These gridded brightness temperatures are produced from swath data obtained from the NOAA Comprehensive Large Array-data Stewardship System (CLASS).

2.2 Derivation Techniques and Algorithms

2.2.1 Overview

NSIDC processes the input brightness temperatures into two different intermediate sea ice concentrations using two GSFC-developed algorithms: NASA Team (Cavalieri et al. 1984) and Bootstrap (Comiso 1986). These intermediate NSIDC NASA Team and Bootstrap sea ice concentrations are used in the NRT NOAA/NSIDC CDR algorithm described in further detail in section 2.2.2 CDR Algorithm.

The passive microwave channels employed for the sea ice concentration product are the 19 GHz, 22 GHz, and 37 GHz frequencies. Table 8 lists the channels used for each algorithm and the channels used for the weather filters. For a complete description of the weather filters, see the Climate Algorithm Theoretical Basis Document (C-ATBD): Passive Microwave Sea Ice Concentration document (Meier, Savoie, and Mallory 2011).

Table 8. NASA Team and Bootstrap Algorithm Channels

	NASA Team	**Bootstrap**
Algorithm Channels	19H, 19V, and 37V	37H, 37V, and 19V
Weather Filters	22V and 19V	22V

Since this data set uses multiple sensors over time, the sea ice algorithms are intercalibrated at the product (concentration) level by NASA GSFC. Thus, the brightness temperature source is less important because the intercalibration adjustment includes any necessary changes due to differences in brightness temperature across them. Both the NASA Team and Bootstrap algorithms employ varying tie-points to account for changes in sensors and spacecraft. These tie-point adjustments are derived from regressions of brightness temperatures during overlap periods. The adjustments are made at the product level by adjusting the algorithm coefficients so that the derived sea ice fields are as consistent as possible.

The NASA Team approach uses sensor-specific hemispheric tie-points for each transition (Cavalieri et al.1999; Cavalieri et al. 2011). Tie-points were originally derived for the SMMR sensor and subsequent transitions to the different SSMIS instruments adjusted the tie-points to be consistent with the original SMMR record. The Bootstrap algorithm uses daily varying hemispheric tie-points, derived via linear regression analysis on clusters of brightness temperature values of the relevant channels (Comiso 2009, Comiso and Nishio 2008). Also, in contrast to the NASA Team, Bootstrap tie-points for SMMR and SSM/I are derived from matching fields from the AMSR-E sensor, which is newer and more accurate.

2.2.2 CDR Algorithm

Different algorithms exist for computing sea ice concentration from brightness temperature data. The two widely used GSFC-developed NASA Team (Cavalieri et al. 1984) and Bootstrap algorithms (Comiso 1986) are describe below. Both of these algorithms have their own inherent advantages and limitations. For this CDR data set, the NASA Team-derived sea ice concentrations are merged with the Bootstrap-derived sea ice concentrations using the CDR algorithm into a single ice concentration estimate. The CDR algorithm steps are as follows:

- First, the sea ice edge is defined using only the Bootstrap-derived data with a 10 percent concentration threshold cutoff. In other words, any grid cell near the ice edge showing a concentration of less than 10 percent in the Bootstrap data is set to open water in the CDR; otherwise it is set to the Bootstrap-derived concentration. Bootstrap is used for the edge because of the ambiguity and potential inconsistencies between how the edge is detected by the NASA Team and Bootstrap algorithms (Meier et al. 2014).

- Second, at each sea ice grid cell within the ice cover, the concentration value given by the NASA Team algorithm and that given by the Bootstrap algorithm are compared; whichever value is greater is selected as the CDR value. This is done because both algorithms tend to underestimate ice concentration, however the source of this bias differs between algorithms (Meier et al. 2014).

The NASA Team algorithm, because it uses a ratio of brightness temperatures, tends to cancel out any physical temperature effects. The Bootstrap algorithm uses relationships between two brightness temperatures that are dependent on physical temperature. Thus, physical temperature changes can affect Bootstrap estimates. Errors occur primarily in regimes with very low temperatures: winter in the high Arctic and near the Antarctic coast (Comiso et al. 1997), where the Bootstrap algorithm can underestimate concentration and give a lower value than the NASA Team algorithm. During winter conditions with more moderate temperatures, NASA Team concentrations also tend to have more of a low bias (Kwok 2002; Meier 2005). During melt conditions, both algorithms tend to underestimate concentration; but the effect is more pronounced in the NASA Team algorithm (Comiso et al. 1997; Meier 2005; Andersen et al. 2007).

While these characteristics of the algorithm are true in an overall general sense, ice conditions and algorithm performance can vary from grid cell to grid cell; and in some cases, this approach of choosing the larger value will result in an overestimation of concentration (Meier 2005). However, using the higher concentration between the two algorithms will tend to reduce the overall underestimation of the CDR estimate (Meier et al. 2014). For a more in-depth discussion on the reasoning behind the algorithm, see the C-ATBD (Meier, Savoie, and Mallory 2011).

2.2.3 NASA Team Algorithm

The NASA Team algorithm uses brightness temperatures from the 19 GHz V, 19 GHz H, and 37 GHz V channels. The methodology is based on two brightness temperature ratios, the polarization ratio (PR) of the 19 GHz V and H channels (Equation 1) and the spectral gradient ratio (GR) of the 19 GHz V and 37 GHz V channels (Equation 2).

$$PR(19) = [T_B(19V) - T_B(19H))]/[T_B(19V) + T_B(19H)]$$ **(Equation 1)**

$$GR(37V/19V) = [T_B(37V) - T_B(19V)]/[T_B(37V) + T_B(19V)]$$ **(Equation 2)**

Where:

Table 9. NASA Team Algorithm Variable Descriptions

Variable	Description
PR(19)	Polarization ratio of the 19 GHz vertical and horizontal channels
$T_B(19V)$	Brightness temperature at the 19 GHz vertical channel

Variable	Description
$T_B(19H)$	Brightness temperature at the 19 GHz horizontal channel
GR(37V/19V)	Gradient ratio of the 37 GHz vertical channel and the 19 GHz vertical channel
$T_B(37V)$	Brightness temperature at the 37 GHz vertical channel

When PR and GR are plotted against each other, brightness temperature values tend to cluster in two locations, an open water (zero percent ice) point and a line representing 100 percent ice concentration, roughly forming a triangle. The concentration of a grid cell with a given GR and PR value is calculated by a linear interpolation between the open water point and the 100 percent line segment. See Figure 1.

For a detailed description of the NASA Team algorithm, please see the Descriptions of and Differences between the NASA Team and Bootstrap Algorithms FAQ and the NASA Technical Memorandum 104647 (Cavalieri et al. 1997), which includes information about differences (for example, tie points) between the original algorithm and the revised NASA Team algorithm, and the NASA Team Algorithm section of the C-ATBD (Meier, Savoie, and Mallory 2011) for a table of tie-point values.

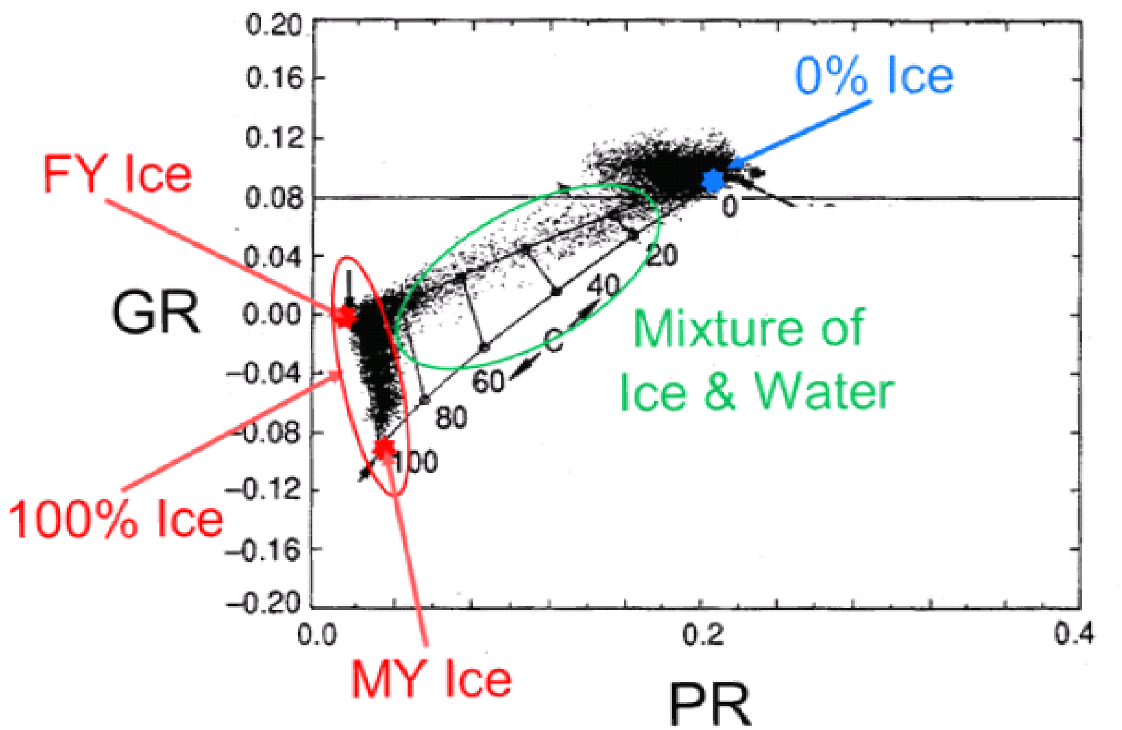

Figure 1. Sample plot of GR vs. PR with typical clustering of grid cell values (small dots) around the 0% ice (open water) point (blue star) and the 100% ice line (circled in red). Points with a mixture of ice and water (circled in green) fall between these two extremes. Adapted from Figure 10-2 of Steffen et al. (1992).

2.2.4 Bootstrap Algorithm

Like the NASA Team algorithm, the Bootstrap algorithm is empirically derived based on relationships of brightness temperatures at different channels. The Bootstrap method uses the fact that scatter plots of different sets of channels show distinct clusters that correspond to two pure surface types: 100 percent sea ice or open water.

Figure 2 shows a schematic of the general relationship between two channels. Points that fall along line segment AD represent 100 percent ice cover. Points that cluster around point O represent open water (zero percent ice). Concentration for a point B is determined by a linear interpolation along the distance from O to I where I is the intersection of segment OB and segment AD. This is described by Equation 3.

$C = (T_B - T_O)/(T_I - T_O)$ **(Equation 3)**

Where:

Table 10. Bootstrap Algorithm Variable Descriptions

Variable	Description
C	Sea ice concentration
T_B	Observed brightness temperature
T_O	Reference brightness temperatures for open water
T_I	Reference brightness temperatures for sea ice

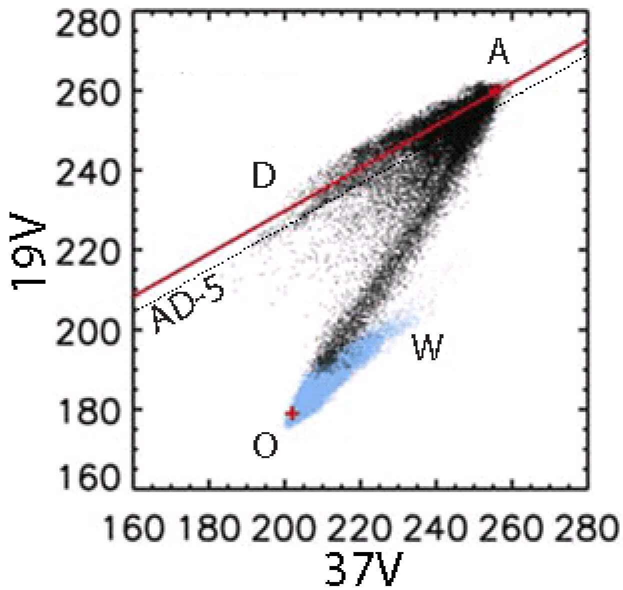

Figure 2. Example of the relationship of the 19V vs. 37V T_B (in Kelvin) used in the Bootstrap algorithm. Brightness temperatures typically cluster around the line segments AD (representing 100% sea ice) and OW (representing 100% open water). For points that fall below the AD-5 line (dotted line), Bootstrap uses T_B relationships for 37H vs. 37V. Adapted from Comiso and Nishio (2008).

The Bootstrap algorithm uses two such combinations, 37 GHz H versus 37 GHz V and 19 GHz V versus 37 GHz V, denoted as HV37 and V1937, respectively. Points that fall within 5 K of the AD segment in a HV37 plot, corresponding roughly to concentrations greater than 90 percent, use this approach. Points that fall below the AD-5 line, use the V1937 relationship to derive the concentration. Slope and offset values for line segment AD were originally derived for each hemisphere for different seasonal conditions (Table 2 in Comiso et al. 1997). However, a newer formulation, employed in this CDR, was developed where slope and offsets are derived for each daily field based on the clustering within the daily brightness temperatures (Comiso and Nishio, 2008). For a detailed description of the Bootstrap algorithm, please see the Descriptions of and Differences between the NASA Team and Bootstrap Algorithms FAQ.

2.3 Processing

Below are the processing steps for both the daily and monthly data files. In addition, the source code is provided for transparency of the algorithm and processes used in creating the NRT sea ice CDR. This source code is for reference only and is not intended to be portable to any computer system beyond that of the original CDR producer's environment. You can access the code from the NOAA Climate Data Record Program's Operation CDR Web page under the Oceanic CDRs section.

2.3.1 Daily Files

The following are the general steps NSIDC uses to produce the daily NRT NOAA/NSIDC CDR sea ice concentration product. See Figure 3 for a diagram of the data flow.

1. Obtain input brightness temperatures from the NSIDC *Near-Real-Time DMSP SSM/I-SSMIS Daily Polar Gridded Brightness Temperatures* (NSIDC-0080) data set. See Table 8 for a list of channels used.
2. Process the brightness temperatures into two intermediate sea ice concentration products using both the NASA Team and Bootstrap algorithms — the two orange objects in the middle blue panel in Figure 3.
3. Merge the intermediate NSIDC NASA Team and Bootstrap data into the NRT CDR using the CDR algorithm and populate the `seaice_conc_cdr` variable.
4. Compute the NRT CDR sea ice concentration standard deviation (`stdev_of_seaice_conc_cdr`) and flag values (`qa_of_seaice_conc_cdr`).
5. Add melt-indicator flag to the QA variable (`qa_of_seaice_conc_cdr`) via a post-processing step.

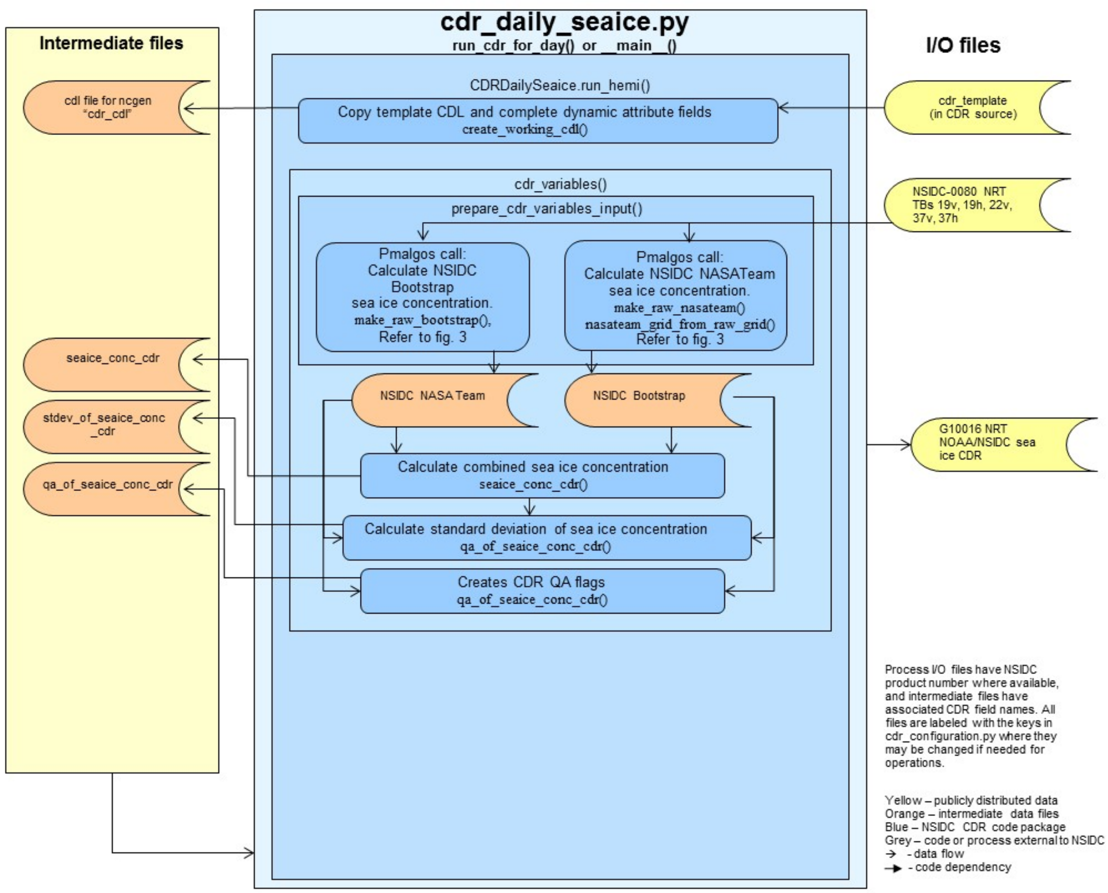

Figure 3. Flow of Data through the Daily NRT CDR Processing.

2.3.2 Monthly Files

The following are the general steps NSIDC uses to produce the monthly NRT NOAA/NSIDC CDR sea ice concentration product. See Figure 4 for a diagram of the data flow.

1. Read the input data: NRT CDR daily sea ice concentration (`seaice_conc_cdr`).
2. Compute the monthly mean concentration for each grid cell for a given month from the daily values.
3. Compute the standard deviation and quality flags.
4. Populate the monthly NetCDF variables and create the files.

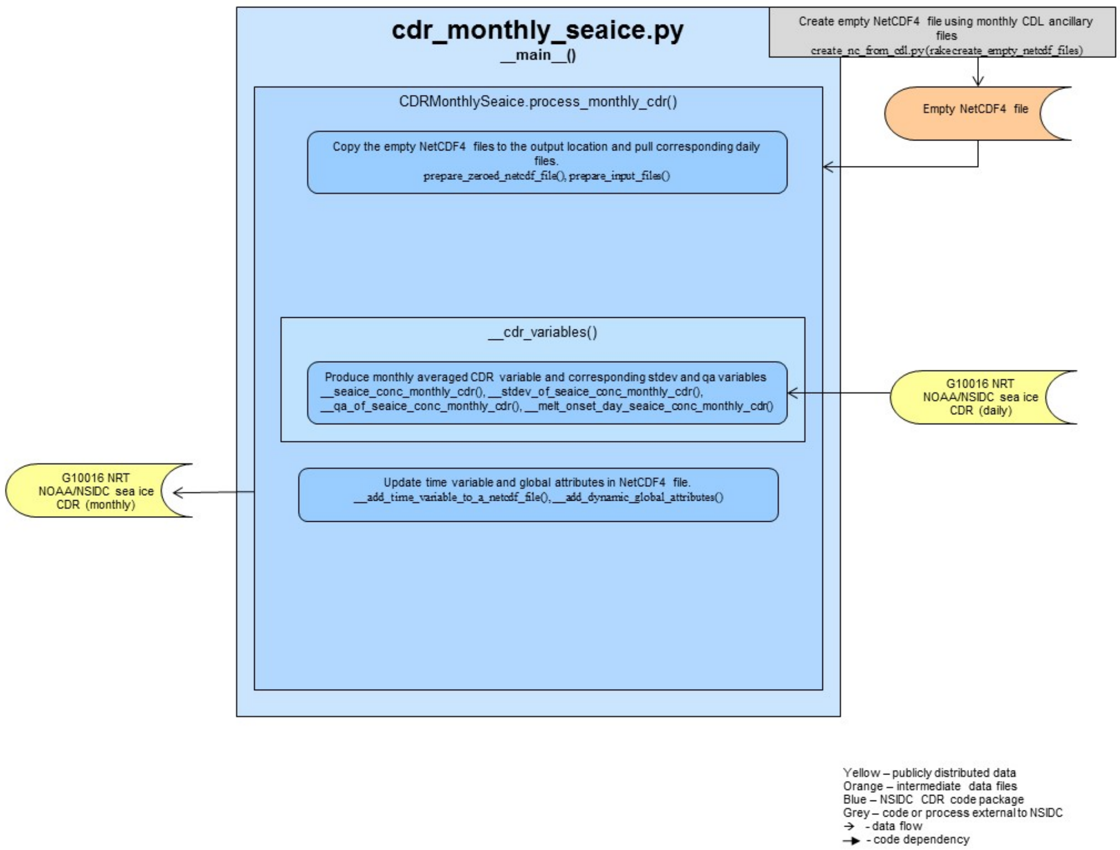

Figure 4. Flow of Data through the Monthly NRT CDR Processing.

2.4 Errors

Several studies over the years have assessed sea ice concentration estimates from the NASA Team and Bootstrap algorithms. These assessments have typically used coincident airborne or satellite remote sensing data from optical, thermal, or radar sensors, generally at a higher spatial resolution than the SSM/I instrument but with only local or regional coverage. Several assessments indicate an accuracy of approximately five percent during mid-winter conditions away from the coast and the ice edge (Steffen et al. 1992; Gloersen et al. 1993; Comiso et al. 1997; Meier et al.

2005; Andersen et al. 2007, Belchansky and Douglas 2002). Other assessments suggest concentration estimates are less accurate. Kwok (2002) found that passive microwave overestimates open water by three to five times in winter. Partington et al. (2003) found a difference with operational charts that was relatively low in the winter, but rose to more than 20 percent in summer.

Researchers can assess and improve a CDR by comparing it with operational products — real-time products that help ships cross the sea ice. Absolute error can be approximated via comparison to operational sea ice products, such as those produced by the U.S. National Ice Center (NIC) or the Canadian Ice Service, but it is important to keep in mind that such products have an operational focus different from the climate focus of the CDR, and the two are not expected to be consistent with each other. The documentation for the daily Multi-sensor Analyzed Sea Ice Extent (MASIE), distributed by NSIDC in cooperation with NIC, gives a summary of how satellite passive microwave CDRs differ from operational products.

Errors can come from problems with the sensor, from weather effects, and from inadequacies in the algorithm. A satellite's orbit may drift over time, for example, which may degrade the data quality of an instrument. Most SSM/I instruments were used long past their designed lifetime expectancy. Atmospheric water vapor is a weather effect that can modulate the passive microwave signature of the surface, particularly at the 19 GHz frequency, causing ice concentration to be overestimated. The emissivity of sea water is generally stable, except under strong winds that cause waves to form. The emissivity of sea ice varies considerably depending on many factors including age, thickness, and surface roughness. When one considers that algorithms must arrive at a single number for ice concentration, taking into account the varying brightness temperatures of all the different surface types that may fill the footprints of the 19 GHz and 37 GHz channels, and that those footprints differ in size and shape across the instrument swath, one can appreciate the difficulty of the problem. Microwave Remote Sensing of Sea Ice, edited F. Carsey, provides a comprehensive overview of the subject (Carsey 1992).

Another potential sensor error results from the transition between sensors on different platforms. The brightness temperature regression and tie-point adjustment corrects for this, though small artifacts remain (Cavalieri et al. 1999; Comiso and Nishio 2008). Comparison of ice extent estimates from sensor overlap periods indicate that the adjustments yield agreements that are on the order of 0.05 percent or less and about 0.5 percent for sea ice area (Cavalieri et al. 1999; Cavalieri et al. 2011). Short overlap periods of early sensor transitions (SMMR to F8 and F8 to F11) may not account for the full seasonal variability (Meier and Khalsa 2011b; Cavalieri et al. 2011) and differences may be higher in some cases. However, differences appear to be well below the sensitivity of the instrument, thus, providing confidence in the robustness of the intercalibrated algorithms through the time series.

When melt ponds form on the surface of ice floes in the summer, the ice concentration appears to decline when in fact the true concentration may not have changed (Fetterer and Untersteiner 1998). Melt state is a surface effect that may in itself contain a climate trend, which could influence sea ice concentration trend estimates. This and other concentration error sources have been examined to some extent in Andersen et al. (2007), and their influence appears to be small compared to the estimated sea ice trends, but such effects should be kept in mind when using these data.

The NetCDF4 files contain a variable called `qa_of_seaice_conc_cdr` to help data users assess the quality of a given data value. Table 3 gives a list of the flags, their values, and their meaning. Values less than eight indicate that conditions for high error are not present — though errors could still be high — and also denotes the algorithm source (NASA Team or Bootstrap) or area covered by a climatological ocean mask or valid ice mask. Values greater than or equal to eight indicate that conditions exist that could increase error, with higher values generally indicating greater uncertainty and hence less confidence in the CDR concentration estimate. **Note**: Grid cells that meet multiple conditions will have a value that is the sum of the values of each individual condition.

For a more complete description of error sources and assessments, see the C-ATBD (Meier, Savoie, and Mallory 2011).

2.5 Instrumentation

For the NRT NOAA/NSIDC CDR data (`seaice_conc_cdr`), NSIDC uses brightness temperatures from SSMIS sensors on the DMSP-F18. Table 11 describes the orbital parameters of DMSP-F18.

Table 11. Orbital Parameters of DMSP-F18

Parameter	Value
Nominal Altitude* (km)	833
Inclination Angle (degrees)	98.6
Orbital Period (minutes)	102
Ascending Node Equatorial Crossing (local time)	8:00 p.m.
Algorithm Frequencies* (GHz)	19.4, 37.0
Earth Incidence Angle* (degrees)	53.1
3 dB Beam Width (degrees)*	1.9, 0.4

*Indicates sensor and spacecraft orbital characteristics of the three sensors used in generating the sea ice concentrations.

Table 12 lists the footprint size of the SSMIS instrument.

Table 12. SSMIS Footprint Size

Frequency (GHz)	SSM/I IFOV (km)
19.350	73 x 45
22.235	73 x 45
37.000	41 x 31

For a complete description of the SSMIS instrument, see the SMMR, SSM/I, and SSMIS Sensors Summary.

3 SOFTWARE AND TOOLS

There are a number of NetCDF file readers available to read/view NetCDF files. For a list of some of these tools, please see the NetCDF Resources at NSIDC: Software and Tools Web page.

4 VERSION HISTORY

Table 13. Version History

Version	Release Date	Description of Changes
v01r00	August 2017	Initial release of the NRT CDR

5 RELATED DATA SETS

- *NOAA/NSIDC Climate Data Record of Passive Microwave Sea Ice Concentration*
- *DMSP SSM/I-SSMIS Daily Polar Gridded Brightness Temperatures*
- *Sea Ice Concentrations from Nimbus-7 SMMR and DMSP SSM/I Passive Microwave Data*
- *Bootstrap Sea Ice Concentrations from Nimbus-7 SMMR and DMSP SSM/I*
- *Multi-sensor Analyzed Sea Ice Extent (MASIE)*
- *Sea Ice Index*
- *AMSR-E/Aqua Daily L3 12.5 km Brightness Temperatures, Sea Ice Concentration, & Snow Depth Polar Grids*
- *AMSR-E/Aqua Daily L3 25 km Brightness Temperatures & Sea Ice Concentration Polar Grids*

6 RELATED WEBSITES

- NOAA's National Climatic Data Center (NCDC) Climate Data Record (CDR) program
- EUMETSAT Ocean & Sea Ice Satellite Application Facility
- Sea Ice Concentration: NOAA/NSIDC Climate Data Record: Provides an overview of the data product's strengths and weaknesses (Meier and NCAR 2014).

7 CONTACTS AND ACKNOWLEDGMENTS

Walt Meier (PI)

Florence Fetterer (Co-I)

Ann Windnagel (Co-I)

National Snow and Ice Data Center (NSIDC)

Boulder, Colorado USA

7.1 Acknowledgments

This project was supported in part by a grant NA07OAR4310056 from the NOAA NCDC Climate Data Record Program. Production of original NASA Team and Bootstrap algorithm estimates supported by the NASA Polar Distributed Active Archive Center. The sea ice concentration algorithms were developed by Donald J. Cavalieri, Josefino C. Comiso, Claire L. Parkinson, and others at the NASA Goddard Space Flight Center in Greenbelt, Maryland, USA.

The production of the NRT NOAA/NSIDC sea ice CDR is managed by Ann Windnagel at NSIDC.

8 REFERENCES

Andersen, S., R. Tonboe, L. Kaleschke, G. Heygster, and L. T. Pedersen. 2007. Intercomparison of Passive Microwave Sea Ice Concentration Retrievals over the High-Concentration Arctic Sea Ice. J. Geophys. Res., 112, C08004, doi:10.1029/2006JC003543.

Belchansky, G. I., and D. C. Douglas. 2002. Seasonal Comparisons of Sea Ice Concentration Estimates Derived from SSM/I, OKEAN, and RADARSAT Data. Rem. Sens. Environ., 81: 67-81.

Carsey, F. D. (Ed.). 1992. Microwave Remote Sensing of Sea Ice. American Geophysical Union, 462 pp.

Cavalieri, D., C. Parkinson, N. DiGirolamo, A. Ivanov (2011). Intersensor calibration between F13 SSM/I and F17 SSMIS for global sea ice data records. *IEEE Geosci. Remote Sens. Lett*., 9(2), 233-236, doi:10.1109/LGRS.2011.2166754.

Cavalieri, D., C. Parkinson, P. Gloersen, J. Comiso, and H. J. Zwally (1999). Deriving Long-term Time Series of Sea Ice Cover from Satellite Passive-microwave Multisensor Data Sets. J. of Geophys. Res., 104(C7):15,803-15,814.

Cavalieri, D. J., C. L. Parkinson. 1997. Arctic and Antarctic Sea Ice Concentrations from Multichannel Passive-Microwave Satellite Data Sets: October 1978 - September 1995 - User's

Guide. NASA Technical Memorandum 104647. NASA Goddard Space Flight Center, Greenbelt, Maryland.

Cavalieri, D. J., P. Gloersen, and W. J. Campbell. 1984. Determination of Sea Ice Parameters with the NIMBUS-7 SMMR. J. Geophys. Res., 89(D4): 5355-5369.

Comiso, J. C. (2009). Enhanced Sea Ice Concentrations and Ice Extents from AMSR-E Data. *J. Rem. Sens. of Japan,* 29(1):199-215.

Comiso, J. C., and F. Nishio. 2008. Trends in the Sea Ice Cover Using Enhanced and Compatible AMSR-E, SSM/I, and SMMR Data. J. of Geophys. Res., 113, C02S07, doi:10.1029/2007JC0043257.

Comiso, J. C., D. Cavalieri, C. Parkinson, and P. Gloersen. 1997. Passive Microwave Algorithms for Sea Ice Concentrations: A Comparison of Two Techniques. Rem. Sens. of the Environ., 60(3):357-384.

Comiso, J. C. 1986. Characteristics of Arctic Winter Sea Ice from Satellite Multispectral Microwave Observations. J. Geophys. Res., 91(C1): 975-994.

Eaton B., J. Gregory, H. Centre, B. Drach, K. Taylor, and S. Hankin. 2010. NetCDF Climate and Forecast (CF) Metadata Conventions Version 1.5. Programs for Climate Model Diagnosis and Intercomparison. 81 pp. http://cf-pcmdi.llnl.gov/documents/cf-conventions/1.5/cf-conventions.pdf. Accessed Sep. 2011.

Fetterer, F., and N. Untersteiner. 1998. Observations of Melt Ponds on Arctic Sea Ice. J. Geophys. Res., 103(C11): 24, 821-24, 835.

Gloersen, P., W. J. Campbell, D. J. Cavalieri, J. C. Comiso, C. L. Parkinson, and H. J. Zwally. 1993. Arctic and Antarctic Sea Ice, 1978-1987: Satellite Passive-Microwave Observations and Analysis. NASA Spec. Publ. 511, 290 pp.

Kwok, R. 2002. Sea Ice Concentration Estimates from Satellite Passive Microwave Radiometry and Openings from SAR Ice Motion. Geophys. Res. Lett., 29(9), 1311, doi:10.1029/2002GL014787.

Meier, W. N. and the National Center for Atmospheric Research (NCAR) Staff (Eds). 2014. "The Climate Data Guide: Sea Ice Concentration: NOAA/NSIDC Climate Data Record." Retrieved 04 June 2015 from https://climatedataguide.ucar.edu/climate-data/sea-ice-concentration-noaansidc-climate-data-record.

Meier, W. N., G. Peng, D. J. Scott, and M. H. Savoie. 2014. Verification of a new NOAA/NSIDC passive microwave sea-ice concentration climate record. Polar Research 33. doi:10.3402/polar.v33.21004.

Meier, W. N., M. Savoie, and S. Mallory. 2011, updated 2019. CDR Climate Algorithm and Theoretical Basis Document: Sea Ice Concentration, Rev. 7. ed. F. Fetterer and A. Windnagel. NOAA NCDC CDR Program.

Meier, W. N., and S. J. S. Khalsa. 2011. Intersensor Calibration between F13 SSM/I and F17 SSMIS Near-Real-Time Sea Ice Estimates. Geoscience and Remote Sensing 49(9): 3343-3349.

Meier, W. N. 2005. Comparison of Passive Microwave Ice Concentration Algorithm Retrievals with AVHRR Imagery in Arctic Peripheral Seas. IEEE Trans. Geosci. Remote Sens., 43(6): 1324-1337.

Partington, K., T. Flynn, D. Lamb, C. Bertoia, and K. Dedrick. 2003. Late Twentieth Century Northern Hemisphere Sea-Ice Record from U.S. National Ice Center Ice Charts. J. Geophys. Res. 108(C11): 3343. doi:10.1029/2002JC001623.

Peng, G., W. N. Meier, D. J. Scott, and M. H. Savoie. 2013. A long-term and reproducible passive microwave sea ice concentration data record for climate studies and monitoring. Earth Syst. Sci. Data 5: 311-318. doi: 10.5194/essd-5-311-2013.

Steffen, K., J. Key, D. J. Cavalieri, J. Comiso, P. Gloersen, K. St. Germain, and I. Rubinstein. 1992. The Estimation of Geophysical Parameters using Passive Microwave Algorithms, in "Microwave Remote Sensing of Sea Ice." F.D. Carsey, ed., American Geophysical Union Monograph 68, Washington, DC:201-231.

National Research Council of the National Academies. 2004. Climate Data Records from Environmental Satellites: Interim Report. National Academies Press, Washington, D.C., 150 pp.

9 DOCUMENT INFORMATION

9.1 Author

A. Windnagel

9.2 Publication Date

August 2017